Molecular Shot Noise, Burst Size Distribution, and Single-Molecule Detection in Fluid Flow: Effects of Multiple Occupancy

Jörg Enderlein,* David L. Robbins, W. Patrick Ambrose, and Richard A. Keller

CST-1, MS M888, Los Alamos National Laboratory, Los Alamos, New Mexico 87545

Received: March 5, 1997; In Final Form: April 16, 1998

We present a new mathematical approach for calculating burst size distributions for the detection of fluorescent molecules introduced into a fluid flow at different rates. The burst size distributions reflect the passage of more than one molecule through the detection volume in close succession. The calculations are based upon a physical model appropriate for the fluorophore phycoerythrin under the conditions of no saturation of excitation, negligible triplet-state dynamics, and negligible detector dead time. The model includes photophysical properties of the fluorophore phycoerythrin (absorption cross section, fluorescence quantum yield, and photostability); diffusion; sample stream hydrodynamics; spatially dependent optical detection efficiency; and excitation laser beam characteristics. Good agreement is found between the mathematical model and experimental results with phycoerythrin.

Introduction

In recent years, the detection and spectroscopy of single molecules has become a routine experimental technique. Especially, the detection of single fluorescent molecules in liquids at room temperature has made big advances.[1−15] The possible applications of single-molecule detection (SMD) in flowing liquids are broad and very promising, ranging from DNA sequencing,[16−20] sizing of DNA fragments,[21−24] genetic screening,[25] and diagnostics[26,27] to the study of single-molecule chemical kinetics[28−31] and the detection of minute amounts of substances.[32,33]

Our experimental setup for the detection of single molecules in fluid flow is shown in Figure 1. Single molecules are injected from a small capillary into the sheath flow of a surrounding larger capillary. Downstream, a laser beam is focused into the capillary for exciting fluorescence from the molecules passing through the probe volume. The resulting bursts of fluorescence photons emitted by a molecule are detected by appropriate, large numerical aperture (NA) detection optics. The optical axis (*x*-axis) is perpendicular to the flow direction (*z*-axis) and to the laser beam (*y*-axis).

In a SMD experiment in fluid flow, one may measure the number of photons counted in consecutive time intervals of a given width. The common way of processing this measured raw data is to first apply a digital filter to smooth the data (see Appendix A). A burst is defined as a peak in the filtered data stream that exceeds a preset threshold. One may then apply a burst-finding algorithm for isolating individual photon bursts, which corresponds to the transit of fluorescing molecules through the detection volume. The total number of raw data counts that occur during the interval for which the filtered data stream exceeds the threshold is termed the burst size. The burst size distribution (BSD) is computed by first applying to the raw data a smoothing and burst-finding algorithm for finding individual fluorescence photon bursts, corresponding to transits of fluorescing molecules through the detection volume (see Appendix), and, second, by building up a histogram of burst sizes.

In a SMD experiment with a single fluorescent molecular species, with good alignment of the experimental system[12,20,34] and with sufficiently low background, one observes a peak expressed in the BSD due to single molecule transits near the middle of the detection volume. If more than one fluorescent molecular species with different fluorescence characteristics is present in the sample stream, one expects to see several peaks in the BSD corresponding to the different molecular species. Thus, it is possible to distinguish different molecular species in the sample stream by their fluorescence intensity characteristics, a task which may be difficult in some bulk measurements. This technique has been successfully applied to the sizing of DNA fragments stained with intercalating dyes.[21−24]

But, another process will also cause multiple peaks in the BSD. For finite concentrations of fluorescent molecules in the sample stream, there exists always a nonvanishing probability that more than one molecule will pass in close succession through the detection volume. This causes additional peaks in the BSD at the position of higher burst size numbers. A related effect was reported by Chen and Dovichi[33] when detecting very small numbers of molecules in capillary electrophoresis. There, the fluctuations in the number of detected photoelectrons due to the fluctuations of the number of molecules in the sampling volume were dubbed "molecular shot noise".

To analyze this situation in more detail, one needs a concise and reliable theoretical description of the experiment, which allows quantitative predictions of the BSD for different concentrations and molecular characteristics. In a recent paper, we introduced a new path integral approach for the computation of the photon detection statistics in SMD experiments.[35] In the present paper, we apply this approach to the computation of BSDs with special emphasis on the effect of multimolecule events, when more than one molecule traverses the detection volume at the same time.

The paper is organized as follows. In section 2, we outline briefly the path integral approach for calculating burst size

* To whom correspondence should be addressed.

S1089-5639(97)00829-3 CCC: $15.00
Published on Web 07/03/1998

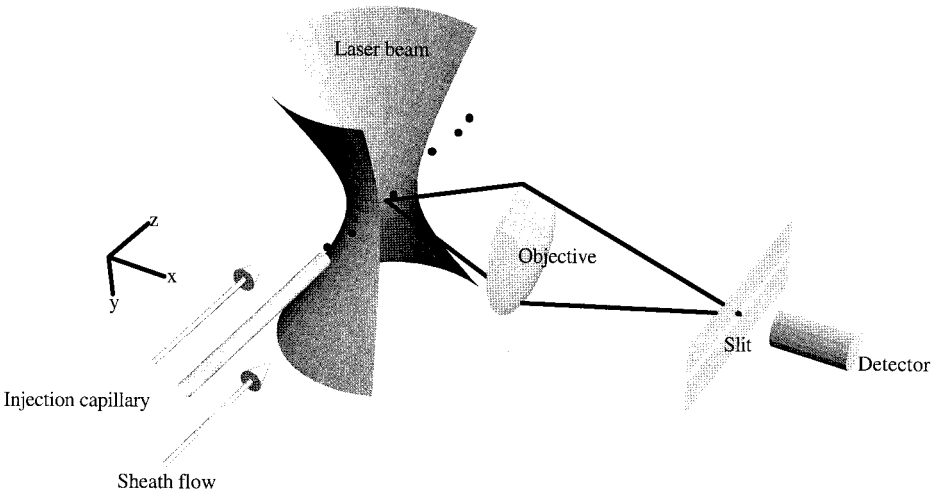

Figure 1. Sheath flow SMD experimental schematic. The coordinate origin is at the focus of the laser beam.

distributions for pure single molecule transits. Furthermore, we consider the problem of multimolecule events from a theoretical point of view. In section 3, we present the results of SMD experiments with B-phycoerythrin and compare the results with the theoretical model developed in section 2. A discussion of the results concludes the paper.

Theoretical Section

Calculating the Burst Size Distribution for Pure Single-Molecule Transits. The experimental setup used in the following considerations is shown in Figure 1. Let us consider the transit of a single molecule through the detection volume. Suppose the molecule starts at $t = 0$ far outside and upstream of the focused laser beam (in some plane $\vec{r}_0 = \{x,y,z_0\}$, $z_0 =$ const.) and choose a time T large enough that the molecule will have crossed the detection volume with near certainty at $t = T$. The BSD is then given by the probability distribution $P_1(N)$ of measuring N photons within the time interval $\{0,T\}$. The lower index 1 reminds us that we are dealing with pure *single*-molecule crossings.

A detailed derivation of the probability distribution $P_1(N)$ is presented in ref 35. Here, we restrict ourselves to conditions corresponding to the SMD experiments with B-phycoerythrin below: no optical saturation effects (low laser intensity); negligible detector and electronic dead times (even for the highest molecule injection rate that we used in our measurements we estimated that we are missing, on average, no more than 3% of the photon counts); linear one-step photobleaching dynamics,[31] and negligible triplet-state dynamics of B-phycoerythrin. Furthermore, we observe no polarization in the emission from phycoerythrin and do not include any polarization effects in the model.

The basic idea is to consider first the subensemble of all molecules with the same trajectory $\vec{r}(t)$ and, among this subensemble, the sub-subensemble of molecules which are photobleached at the same time t_{bl}. For this sub-subensemble of molecules, the photon detection statistics are given by a simple Poisson distribution with a mean equal to

$$V_f = \int_0^{t_{bl}} dt\, V_f[\vec{r}(t)] \tag{1}$$

where $\delta t V_f(\vec{r})$ is the probability of detecting a photon within time δt if the molecule is at position $\vec{r}$. Thus, the probability $P_1(N)$ to detect N photons during the time interval $\{0,T\}$ is a superposition of Poisson distributions,

$$P_1(N) = \int_0^\infty dV_f \frac{V_f^N}{N!} \exp(-V_f) \cdot P[V_f] \tag{2}$$

The distribution function $P[V_f]$ is given in the form of a path integral, running over all possible photobleaching times and molecule trajectories:

$$\begin{aligned} P(V_f) = & \\ & \int_0^T dt_{bl} \int D\vec{r}(t)\, \delta[V_f - \int_0^{t_{bl}} dt V_f[\vec{r}(t)]] V_{bl}[\vec{r}(t_{bl})] \times \\ & \exp\left[-\int_0^{t_{bl}} dt \left(\frac{[\vec{r}(t) - \vec{v}]^2}{4D} + V_{bl}[\vec{r}(t)]\right)\right] p_0[\vec{r}_0] + \\ & \int D\vec{r}(t)\, \delta[V_f - \int_0^T dt V_f[\vec{r}(t)]] \times \\ & \exp\left[-\int_0^T dt \left(\frac{[\vec{r}(t) - \vec{v}]^2}{4D} + V_{bl}[\vec{r}(t)]\right)\right] p_0[\vec{r}_0] \end{aligned} \tag{3}$$

where $\delta[f(\vec{r})]$ is a δ-function functional, $p_0(\vec{r}_0)\ \delta\vec{r}$ is the probability of finding a molecule in the small volume $\delta\vec{r}$ at position $\vec{r}_0$ at time $t = 0$, $\delta t V_{bl}(\vec{r})$ is the probability of photobleaching the molecule within time δt if the molecule is at position $\vec{r}$, D is the diffusion constant of the molecule, and $\vec{v}$ is the flow velocity of the sample stream. The expression $\int D\vec{r}(t)$ symbolizes the path integration, which, in eq 3, runs over all possible paths with arbitrary starting point $\vec{r}_0$ and arbitrary end point. The first term in the sum of eq 3 takes into account the contribution of molecules that photobleach while crossing the laser beam, whereas the second term accounts for all molecules that do not photobleach.

The functions $V_f(\vec{r})$ and $V_{bl}(\vec{r})$ can be specified further by

$$V_f(\vec{r}) = \eta(\vec{r})\, \Phi_f \sigma I(\vec{r}) \tag{4}$$

and by

$$V_{bl}(\vec{r}) = \Phi_{bl} \sigma I(\vec{r}) \tag{5}$$

where $I(\vec{r})$ is the position-dependent laser intensity (photons per area per time), $\eta(\vec{r})$ is the position-dependent collection and detection efficiency of the detection optics and electronics, Φ_f and Φ_{bl} are the fluorescence and photobleaching quantum yields, and σ is the absorption cross section. Here, the laser intensity is assumed to be low (no optical saturation effects), and background counts are neglected. We are not considering background effects here, since fluctuations in the background

in the SMD data could be effectively reduced by the application of a Lee filter.

In general, it is probably impossible to find an analytical expression for $P_1(N)$. In the present paper we apply a Monte-Carlo sampling for calculating the $P_1(N)$. The basic difficulty in calculating eq 3 is that the path integral runs over an infinite number of paths. The idea of a Monte-Carlo calculation is to choose these paths randomly and then to perform the remaining integrations numerically. After sampling over a large number of different paths one expects to gain a sufficiently precise approximation of the true values of $P_1(N)$ (for details see ref 35).

Multiple Molecule Events. For any nonvanishing concentration of fluorescent molecules in the sample stream, the probability that two or more molecules pass in close a succession through the detection volume so as to yield a single photon burst can never be zero. If two (or more) molecules are following in too close a succession, they will cause a single, longer lasting fluorescence burst which is no longer resolvable into two (or more) single bursts (see the Appendix for the burst determination algorithm). This will cause additional peaks in the BSD or at least a broadening of the BSD at higher burst sizes. To model this, we will use a simplified picture. Let w_k be a weight factor proportional to the probability that k molecules pass successively through the detection volume each separated by less than the mean transit time, producing a single unresolved burst. The corresponding BSD of all such k-molecule bursts is then given by the convolution of the BSD for all $(k-1)$-molecule bursts with the BSD of pure single-molecule bursts. Thus, for the two-molecule BSD we have

$$P_2(N) = \sum_{N_1+N_2=N} P_1(N_1)\, P_1(N_2) \tag{6}$$

and for the k-molecule BSDs with $k > 2$

$$P_k(N) = \sum_{N_1+N_2+\ldots+N_k=N} P_1(N_1)\, P_1(N_2)\ldots P_1(N_k)$$

$$= \sum_{N_1+N_2=N} P_1(N_1) P_{k-1}(N_2) \tag{7}$$

An estimate for the weight factors w_k remains to be found. Let τ_s be the minimum time between molecules which will yield resolvable photon bursts, and τ_m be the mean delivery time between molecules injected into the fluid flow (molecule delivery rate equal to $1/\tau_m$). Then w_k can be calculated as being proportional to the probability that k successive molecules are separated by times less than τ_s and that before and after this "molecular train" there is no other molecule within time τ_s. If molecules are assumed to arrive randomly, then the probability density of the time t until the next molecule arrival is τ_m^{-1} $\exp(t/\tau_m)$. Thus, the probability that $t > \tau_s$ is given by $\exp(-\tau_s/\tau_m)$, and we have for the w_k

$$w_k = \exp\left(-\frac{\tau_s}{t_m}\right)\left[\prod_{j=1}^{k-1}\int_0^{\tau_s}\frac{dt_j}{\tau_m}\exp\left(-\frac{t_j}{\tau_m}\right)\right]\exp\left(-\frac{\tau_s}{\tau_m}\right)$$

$$= \exp\left(-\frac{2\tau_s}{t_m}\right)\left[1-\exp\left(-\frac{\tau_s}{t_m}\right)\right]^{k-1} \tag{8}$$

This, of course, is only an approximate estimation since it assumes a constant value of τ_s for all bursts. A similar estimate for the case $k = 2$ is given in ref 36.

Experimental Section

The experimental apparatus used to collect the B-phycoerythrin data is similar to that previously used for DNA fragment sizing.[22−24] Excitation was accomplished with a mode-locked (200 ps pulse width @ 82 MHz) Ar^+ laser operated at 514.5 nm. The output was attenuated with a polarizer/half-wave plate assembly to 1.0 mW and focused to a 20 μm ($1/e^2$ diameter) circular spot at the center of a 250 × 250 μm^2 square bore sheath flow cuvette (NSG Precision Cell, Inc.). Fluorescence was collected at 90° with a 40×, 0.85 NA microscope objective (Nikon Fluor) and spatially filtered with a 400 μm slit located at the image plane of the microscope objective. The probe volume thus defined was approximately 3 pL. Light passing through the slit was spectrally filtered with a 30 nm bandpass filter centered at 575 nm (575DF30 Omega Optical). The filtered light was focused with a 10× microscope objective on the 200 × 200 μm^2 area of a photon-counting avalanche photodiode (SPCM-200-PQ C.D. 2027, EG&G Optoelectronics, Canada). The sheath fluid water was deionized and purified on a Milli-Q water system (Millipore, Bedford, MA) and was delivered to the flow cell using gravity feed. The sheath volumetric flow rate was adjusted to give transit times through the probe of ca. 1 ms. B-phycoerythrin dissolved in 1× Dulbecco's phosphate buffered saline at a concentration of 1.4×10^{-10} M was forced through a capillary (o.d. 90 μm, i.d. 20 μm, Polymicro Technologies) via a pressure differential. B-Phycoerythrin was eluted from the capillary tip, which was positioned inside the square bore cuvette, approximately 100 μm upstream of the probe volume.

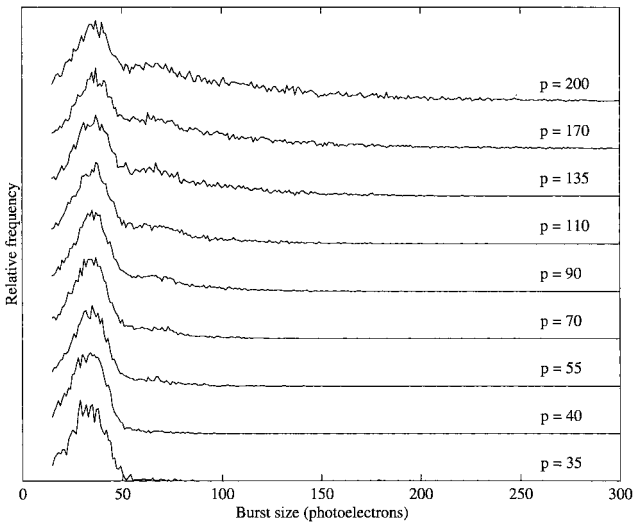

Figure 2. Measured B-phycoerythrin BSDs for different injection pressures (numbers on the right side in units of mmHg). The distributions were calculated from a total of between 1700 (lowest injection rate) and 9000 (highest injection rate) bursts. The curves are offset from each other for clarity.

Photoelectron pulses from the photodiode were amplified, conditioned with a constant fraction discriminator, and counted with a multichannel scaler (MCS) PC card (Oxford Instruments). An IDL (Interactive Data Language, Research Systems, Inc.) program was used to analyze the data (see Appendix). Photon bursts from B-phytocoerythrin were sifted from the data, and the burst areas were integrated and histogramed.

The BSDs of nine measurements at different injection rates (different injection pressures) are shown in Figure 2. The sheath flow velocity was held constant throughout these measurements to yield a transit time of ca. 1 ms. At low sample injection pressure, the B-phycoerythrin molecules are dilute enough that mostly single molecules pass through the focused laser and a single peak appears at 30 photoelectrons. With increasing

injection rate, additional features occur in the high burst size region, which indicates an increasing fraction of multimolecule bursts.

Results

Before being able to perform numerical calculations of the BSDs, one has to specify the spatially dependent laser beam intensity $I(\vec{r})$, the spatially dependent optical collection efficiency $\eta(\vec{r})$, and the initial molecule distribution $p_0(\vec{r})$. For the laser beam intensity we assumed a Gaussian profile (laser focus situated at $x = z = 0$).

$$I(x,z) = \frac{2P_0}{\pi\omega^2}\exp\left[-2\frac{x^2+z^2}{\omega^2}\right] \tag{9}$$

where ω denotes the beam waist radius and P_0 is the total laser power (in photons per time unit). We neglect the divergence of the beam, assuming that the extent of the detection region along the laser beam is sufficiently small.

For the optical collection efficiency we used the expressions derived and studied in ref 37. With η_0 denoting the maximum value of the collection efficiency and d being the width of the slit image in the object space, the spatial dependence of the collection efficiency function $\eta(\vec{r})$ is given by

$$\eta(x,y) = \frac{\eta_0}{\pi(1-\cos\psi)} \times \left[\arcsin\left(\frac{\sin\theta}{\sin\psi}\right) - \cos\psi\arctan\left(\frac{\cos\psi\sin\theta}{\sqrt{\sin^2\psi - \sin^2\theta}}\right)\right]_{\theta_{\min}}^{\theta_{\max}} \tag{10}$$

where the abbreviations

$$\psi = \arcsin(\mathrm{NA}/n)$$

$$\theta_{\min} = \max\left(-\arctan\left(\frac{d/2+y}{|x|}\right), -\psi\right) \tag{11}$$

$$\theta_{\max} = \min\left(\arctan\left(\frac{d/2-y}{|x|}\right), -\psi\right)$$

are used, and $\theta_{\min} < \theta_{\max}$. NA is the value of the numerical aperture, and n is the refractive index in the object space. If $\theta_{\min} > \theta_{\max}$, then $\eta(x,y)$ is equal to zero.

The initial probability $p_0(\vec{r}_0)$ is assumed to be uniform at the injection capillary. Rather than running the Monte-Carlo simulation the entire distance to the laser focus, we recalculated the distribution at a new position $z = z_0$ upstream of the laser focus, employing the simple hydrodynamic model from ref 35. The optics were adjusted to obtain a narrow burst size distribution, i.e., optimal alignment. Thus, the molecules are eluted from the injection capillary at position $z = z_0$ with a uniform distribution over some disk $x^2 + y^2 \le R^2$. The sample is then accelerated to the sheath flow velocity and undergoes diffusion. The starting plane for the Monte-Carlo simulations was chosen to be at $z = z_0 = -3\omega$ (negligible light intensity at this point). Then the initial molecule distribution is given by

$$p_0(x,y,z) = \frac{\delta(z-z_0)}{4\pi^2R^2Dt_0}\int_0^R \mathrm{d}r\, r\int_0^{2\pi}\mathrm{d}\phi \times \exp\left[-\frac{(x-r\cos\phi)^2 + (y-r\sin\phi)^2}{4Dt_0}\right] \tag{12}$$

where D is the diffusion constant, and t_0 is indirectly determined by the equation

$$\frac{z_0 - z_{\mathrm{inj}}}{v_0} = t_0 - \frac{1}{\kappa}[1 - \exp(-\kappa t_0)] \tag{13}$$

where v_0 denotes the flow velocity and κ is some empirical flow acceleration constant. It is assumed that the extent of the lateral distribution (across the flow direction) of the molecules is small enough so that any effect of the velocity profile of the sheath flow can be neglected. Furthermore, the sample stream is assumed to be exactly centered with respect to the laser beam axis and the optical collection axis.

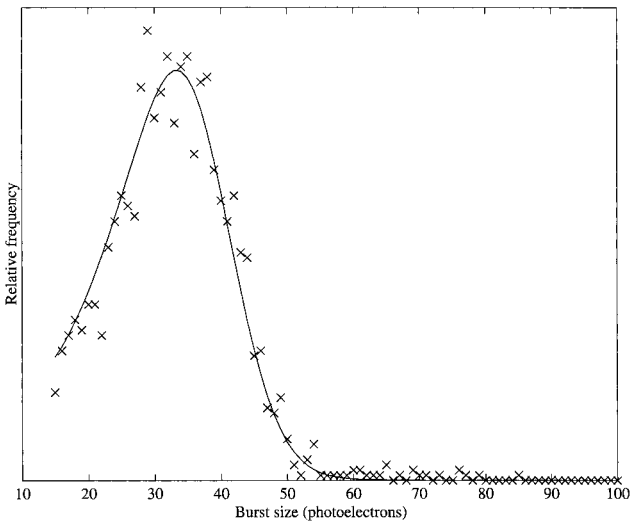

Figure 3. Comparison between measured (crosses) and calculated pure single-molecule (solid line) BSD for the lowest injection rate (35 mmHg).

The following parameter values were used throughout all calculations (see ref 35): diffusion constant $D = 43\ \mu\mathrm{m}^2/\mathrm{s}$, absorption cross section $\sigma = 5.4 \times 10^{-7}\ \mu\mathrm{m}^2$, fluorescence quantum yield $\Phi_f = 0.98$, total laser power $P_0 = 2.6 \times 10^{15}\ \mathrm{s}^{-1}$ (1.0 mW @ 514 nm), laser beam waist radius $\omega = 10\ \mu\mathrm{m}$, width of the slit image in the object space $d = 10\ \mu\mathrm{m}$, maximum collection efficiency $\eta_0 = 1.3 \times 10^{-2}$, and distance of the injection point from the laser beam $z_{\mathrm{inj}} = -100\ \mu\mathrm{m}$.

The time step used in the Monte-Carlo simulation was $\Delta t = 50\ \mu\mathrm{s}$ (equal to the time bin width in the experimental measurement system), and T was set equal to 2.5 ms. For every simulation, 10^4 paths were sampled. One simulation requires approximately 3.5 min on a Pentium processor 133 MHz PC. The simulation program was written with Matlab and can be requested from the authors.[38]

To obtain the pure single-molecule BSD, $P_1(N)$, four unknown parameters were adjusted: the photobleaching quantum yield Φ_{bl}, the flow velocity v_0 (assumed to be uniform over the detection region), the disk radius R, and the acceleration parameter κ. First, we modeled the BSD with the lowest injection pressure and thus the smallest fraction of non-single-molecule crossings. From a fit to the data (Figure 2, $p = 35$ mmHg) we find $\Phi_{bl} = 6 \times 10^{-5}$, $v_0 = 2.4$ cm/s, $R = 5\ \mu\mathrm{m}$, and $\kappa = 175\ \mathrm{s}^{-1}$. The comparison between the fit result and experiment is shown in Figure 3.

To account for multimolecule burst events, we calculated the higher distributions $P_k(N)$ according to eqs 6 and 7 for $k = 2, \ldots, 7$. We fitted the ratio τ_s/τ_m directly to the data via eqs 6−8 using a nonlinear least-squares fitting algorithm. The fit of the burst size distribution for the highest injection rate is shown in Figure 4. Figure 5 shows the dependence of the fitted ratio

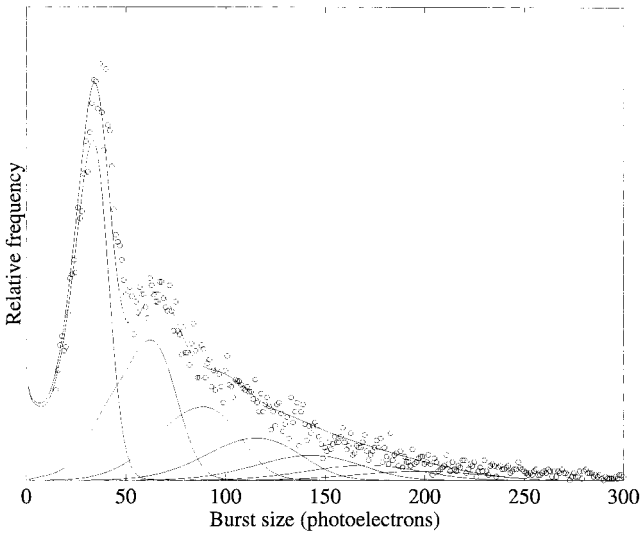

Figure 4. Comparison between measured (circles) and calculated (upper solid line) BSD for the highest injection rate. In the calculation, the distributions $P_k(N)$ were calculated for $k = 2, ..., 7$ from $P_1(N)$ shown in Figure 3. The amplitudes of each P_k were calculated according to eqs 8. The component distributions are shown as solid lines. The increase in burst frequency in the model calculations near the origin reflects the influence of photobleaching, leading to a larger frequency of small bursts.

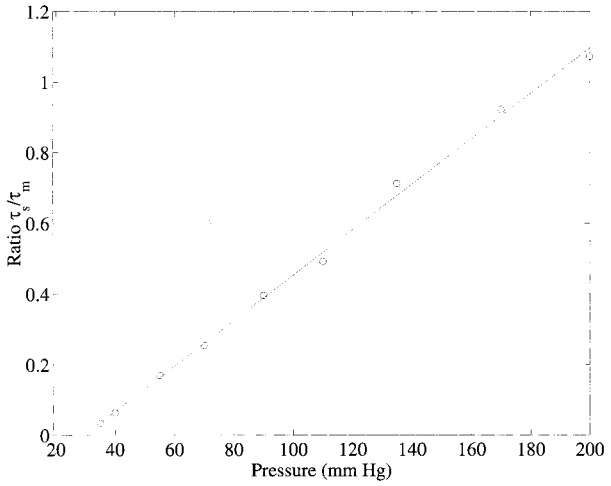

Figure 5. Linear fit of the τ_s/τ_m values versus the injection pressure.

τ_s/τ_m on the sample injection pressure. Theoretically, the injection rate (and thus τ_s/τ_m) should be directly proportional to the injection pressure:

$$\frac{\tau_s}{\tau_m} = c(\pi - \pi_0) \tag{14}$$

where π is the injection pressure, π_0 is a pressure offset value, and c is a constant factor.

Discussion

Taking into account the noise in the measured BSDs, and the simplicity of the assumptions leading to eqs 6−8, the linearity of the correlation between the determined ratios of τ_s/τ_m and the injection pressure as shown in Figure 5 is encouraging. Thus, it is possible to extract information about the molecule injection rate directly from the BSD. Furthermore, predicting the exact BSD will be important in the evaluation of SMD data where more than only one fluorescent molecular species is present. Then, one has to distinguish between contributions caused by multiple-molecule events of a single-molecular species and single-molecular events of species with different values of the product of the absorption cross section and fluorescence quantum yield.

It should be emphasized that the method presented for determination of the ratio τ_s/τ_m (proportional to the molecule injection rate) from the BSD is quite general. Even if one is not able to calculate theoretically the pure single-molecule BSD, $P_1(N)$, one can use the measured distribution (in the low injection rate limit) to build up, by the simple convolutions of eqs 6 and 7, the higher order BSDs, $P_k(N)$. The ratio τ_s/τ_m was determined via a nonlinear fit, following eq 8. This is especially useful for obtaining accurate values of τ_s/τ_m under conditions of high injection rate. In this sense, measuring carefully the pure single molecule BSD $P_1(N)$ provides a kind of instrumental response function, from which the ratio τ_s/τ_m for any other BSD can be determined.

Acknowledgment. We thank Peter M. Goodwin (LANL) for many helpful discussions. We are grateful to Robert Habbersett (LANL) for providing us with the IDL burst sifting routine. J.E. greatly acknowledges the support of the German Academic Exchange Service, granting him his stay with the Los Alamos National Laboratory. J.E. thanks also Edgar Klose (GMBU e.V. Berlin) for the great support of his work.

Appendix: Burst-Finding Algorithm

The raw data n_k (the number of photoelectrons in bin k, $1 \le k \le N$) were smoothed by a Lee filter. Ideally, every burst consists of a gradual increase and decrease of photocounts. But Poissonian fluctuations lead to the effect that the number of photocounts can be below a chosen threshold even after the beginning or before the end of a burst. Then, the edges of the burst are not recognized as belonging to the same burst, but are recognized as separate bursts. This leads to underestimates of burst sizes at high burst size numbers and to a tremendous increase in the number of apparent bursts with low burst size numbers. The function of the Lee filter is to smooth the data and thus to preclude a distortion of the burst size distribution when applying a simple threshold procedure.

A Lee filter of window width $2m + 1$ is defined as follows: First, a running mean and variance are calculated using

$$\bar{n}_k = \frac{1}{(2m+1)} \sum_{j=-m}^{m} n_{k+j}, \quad m < k \le N - m$$

$$\sigma_k^2 = \frac{1}{(2m+1)} \sum_{j=-m}^{m} (n - \bar{n})_{k+j}^2, \quad 2m < k \le N - 2m \tag{A1}$$

The range of k values is limited by the window width. The filtered data $\tilde{n}_k$ are given by

$$\tilde{n}_k = \bar{n}_k + (n_k - \bar{n}_k)\frac{\sigma_k^2}{\sigma_k^2 + \sigma_0^2} \tag{A2}$$

where σ_0 is some constant, characterizing the filter. The resulting smoothed data $\tilde{n}_k$ are used to define a photoelectron burst. A burst is defined by any continuous number of bins with $\tilde{n}_k > n_{th}$, where n_{th} is a predefined threshold value. The value of n_{th} was set equal to 1.5 times the estimated mean background count number. For the determination of the burst size itself, the raw data count numbers n_k are summed up over

the burst range. For our experimental data, the width of the Lee filter window was set to be $2m + 1 = 11$ ($m = 5$), and the value of σ_0 was always equal to 5.

It should be noted that an increasing value of m increases the value of τ_s. Since τ_s increases with m, a larger fraction of multiple-molecule bursts are sifted from the data with increasing m. We performed the data analysis leading to Figure 5 for values of m between $m = 3$ and $m = 7$, and we found a nearly linear dependence of the slope $c = (\tau_s/\tau_m)/(\pi - \pi_0)$ (see eq 14) that can be expressed as $c = (0.3 + 3m) \times 10^{-3}$ (mmHg)$^{-1}$, reflecting the increasing value of τ_s with increasing m.

References and Notes

(1) Shera, E. B.; Seitzinger, N. K.; Davis, L. M.; Keller, R. A.; Soper, S. A. *Chem. Phys. Lett.* **1990**, *174*, 553.

(2) Soper, S. A.; Shera, E. B.; Martin, J. C.; Jett, J. H.; Hahn, J. H.; Nutter, H. L.; Keller, R. A. *Anal. Chem.* **1991**, *63*, 432.

(3) Whitten, W. B.; Arnold, J. M.; Ramsey, J. M.; Bronk, B. V. *Anal. Chem.* **1991**, *63*, 1027.

(4) Soper, S. A.; Davis, L. M.; Shera, E. B. *J. Opt. Soc. Am. B* **1992**, *9*, 1761.

(5) Soper, S. A.; Mattingly, Q. L.; Vegunta, P. *Anal. Chem.* **1993**, *65*, 740.

(6) Wilkerson, C. W.; Goodwin, P. M.; Ambrose, W. P.; Martin, J. C.; Keller, R. A. *Appl. Phys. Lett.* **1993**, *62*, 2030.

(7) Rigler, R.; Widengren, J.; Mets, Ü. *Fluorescence Spectroscopy*; Wolfbeis O. S., Ed.; Springer: Berlin, 1993; pp 13−24.

(8) Lee, Y. H.; Maus, R. G.; Smith, B. W.; Winefordner, J. D. *Anal. Chem.* **1994**, *66*, 4142.

(9) Mets, Ü.; Rigler, R. *J. Fluoresc.* **1994**, *4*, 259.

(10) Nie, S.; Chiu, D. T.; Zare, R. N. *Science* **1994**, *266*, 1018.

(11) Nie, S.; Chiu, D. T.; Zare, R. N. *Anal. Chem.* **1995**, *67*, 2849.

(12) Li, L.-Q.; Davis, L. M. *Appl. Opt.* **1995**, *34*, 3208.

(13) Barnes, M.D.; Whitten, W.B.; Ramsey J.M. *Anal. Chem.* **1995**, *67*, 418A.

(14) Goodwin, P. M.; Affleck, R. L.; Ambrose, W. P.; Jett, J. H.; Johnson, M. E.; Martin, J. C.; Petty, J. T.; Schecker, J. A.; Wu, M.; Keller, R. A. *Computer Assisted Analytical Spectroscopy*; Brown S. D., Ed.; John Wiley and Sons: New York, in press.

(15) Keller, R. A.; Ambrose, W. P.; Goodwin, P. M.; Jett, J. H.; Martin, J. C.; Wu, M. *Appl. Spectrosc.* **1996**, *50*, 12A.

(16) Jett, J. H.; Keller, R. A.; Martin, J. C.; Marrone, B. L.; Moyzis, R. K.; Ratliff, R. L.; Seitzinger, N. K.; Shera, E. B.; Stewart, C. C. *J. Biomol. Struct. Dyn.* **1991**, *7*, 301.

(17) Harding, J. D.; Keller, R. A. *Trends Biotechnol.* **1992**, *10*, 55.

(18) Ambrose, W. P.; Goodwin, P. M.; Jett, J. H.; Johnson, M. E.; Martin, J. C.; Marrone, B. L.; Schecker, J. A.; Wilkerson, C. W.; Keller, R. A.; Haces, A.; Shih, P.-J.; Harding, J. D. *Ber. Bunsen-Ges. Phys. Chem.* **1993**, *97*, 1535.

(19) Goodwin, P. M.; Schecker, J. A.; Wilkerson, C. W.; Hammond, M. L.; Ambrose, W. P.; Jett, J. H.; Martin, J. C.; Marrone, B. L.; Keller, R. A. *Proc. SPIE* **1993**, *1891*, 127.

(20) Goodwin, P. M.; Affleck, R. L.; Ambrose, W. P.; Demas, J. N.; Jett, J. H.; Martin, J. C.; Reha-Krantz, L. J.; Semin, D. J.; Schecker, J. A.; Wu, M.; Keller, R. A. *Exp. Tech. Phys.* **1995**, *41*, 279.

(21) Castro, A.; Fairfield, F. R.; Shera E. B. *Anal. Chem.* **1993**, *65*, 849.

(22) Goodwin, P. M.; Johnson, M. E.; Martin, J. C.; Ambrose, W. P.; Marrone, B. L.; Jett, J. H.; Keller, R. A. *Nucleic Acids Res.* **1993**, *21*, 803.

(23) Petty, J. T.; Johnson, M. E.; Goodwin, P. M.; Martin, J. C.; Jett, J. H.; Keller, R. A. *Anal. Chem.* **1995**, *67*, 1755.

(24) Huang, Z.; Petty, J. T.; O'Quinn, B.; Longmire, J. L.; Brown, N. C.; Jett, J. H.; Keller, R. A. *Nucleic Acids Res.* **1996**, *24*, 4202.

(25) Castro, A.; Shera, E. B. *Appl. Opt.* **1995**, *34*, 3218.

(26) Eigen, M.; Rigler, R. *Proc. Natl. Acad. Sci. U.S.A.* **1994**, *91*, 5740.

(27) Rigler, R. *J. Biotechnol.* **1995**, *41*, 177.

(28) Xue, Q.; Yeung, E. S. *Nature* **1995**, *373*, 681.

(29) Wang, J.; Wolynes, P. *Phys. Rev. Lett.* **1995**, *74*, 4317.

(30) Edman, L.; Mets, U.; Rigler, R. *Proc. Natl. Acad. Sci. U.S.A.* **1996**, *93*, 6710.

(31) Wu, M.; Goodwin, P. M.; Ambrose, W. P.; Keller, R. A., *J. Phys. Chem.* **1996**, *100*, 17406.

(32) Chen, D. Y.; Adelhelm, K.; Cheng, X. L.; Dovichi, N. J. *Analyst* **1994**, *119*, 349.

(33) Chen, D. Y.; Dovichi, N. J. *Anal. Chem.* **1996**, *68*, 690.

(34) Goodwin, P. M.; Ambrose, W. P.; Keller R. A. *Acc. Chem. Res.*, in press.

(35) Enderlein, J.; Robbins, D. L.; Ambrose, W. P.; Goodwin, P. M.; Keller R. A. *J. Phys. Chem.* **1996**, *101*, 3626.

(36) Lindmo, T.; Peters, D. C.; Sweet R. G. *Flow Cytometry and Sorting*; Melamed, M. R., Lindmo, T., Mendelsohn, M. L., Eds.; Wiley-Liss: New York, 1990; pp 145−69.

(37) Enderlein, J.; Ambrose W. P. *Appl. Opt.* **1997**, *36*, 5298.

(38) A *Matlab* program code of the Monte-Carlo sampling can be obtained from the authors by sending an e-mail to joerg.enderlein@chemie.uni-regensburg.de. *Matlab* is a registered trademark by MathWorks Inc.